

Optimization of active regions in midinfrared lasers

J. T. Olesberg,^{a)} Michael E. Flatté,^{a),b)} and B. J. Brown^{a)}
Optical Science and Technology Center, University of Iowa, Iowa City, Iowa 52242

C. H. Grein
Department of Physics, University of Illinois, Chicago, Illinois 60607

T. C. Hasenberg,^{a)} S. A. Anson,^{c)} and Thomas F. Boggess^{a),c)}
Optical Science and Technology Center, University of Iowa, Iowa City, Iowa 52242

(Received 10 June 1998; accepted for publication 28 October 1998)

The ideal performance of bulk, quantum well, and superlattice active regions for III–V interband midinfrared lasers are compared according to the maximum net gain per unit current density. Based on this figure of merit, which is appropriate for high-power as well as near-threshold operation, InAsSb quantum well active regions should have an order of magnitude lower threshold current than bulk InAs at room temperature. Optimized four-layer superlattices based on the InAs/GaInSb material system, however, should have two to ten times lower threshold currents than the quantum well active regions. Optimal thicknesses for these active regions were evaluated assuming a separate confinement region design. For the four-layer superlattices the optimal thickness is substantially thinner than has been commonly grown: 3 periods rather than 40 periods. © 1999 American Institute of Physics. [S0003-6951(99)01601-0]

Active regions in current III–V semiconductor lasers emitting in the 3–5 μm range have been grown from a wide variety of material systems. There are type I interband lasers, such as InAsSb/AlAsSb,¹ InAsSb/InAsP,² or InSb/AlInSb,³ and type II broken-gap lasers, either in traditional^{4,5} or cascade configuration,⁶ and intersubband cascade lasers.⁷ While a variety of claims have been made in these works and others concerning the relative *ideal* performance of these systems, evaluation of these claims have been hampered by the lack of a common figure of merit. As an example, consider Auger coefficients: different conventions seem appropriate for superlattices and quantum wells (i.e., whether the barrier region is included in the definition of the carrier density). A more appropriate quantity used for evaluation has been the volumetric threshold current density for a particular gain,^{8,9} but that is not flexible enough to compare laser designs based on different thicknesses of the active region.

An appropriate figure of merit is required that can be used to compare quantum well, superlattice, and bulk active region lasers. To be most useful, this figure of merit should be applicable whether the laser design is for high-power or low-threshold operation. Ideally, it would even allow fair comparison between traditional and cascade structures. Such a figure of merit has been used in the context of near-infrared lasers for some time,¹⁰ and appropriately weighs the importance to laser performance of the density of states, recombination rates, differential gain, and intersubband absorption within the active region. This figure of merit is the maximum net material gain to *volumetric* current density ratio $[(\gamma - \alpha_a)/J]_{\text{max}}$ of the active region. Here γ and α_a are the material gain and absorption, and J is the volumetric current density, all within the active region.

Given a particular laser cavity design, the current (I) for a given output power (P_o) depends on the net gain to current density ratio according to the equation

$$I = \frac{AD_{\text{mode}}(\alpha_m + \langle\alpha_w\rangle)}{\eta_i} \left(\frac{J}{\gamma - \alpha_a} \right) + \frac{eP_o}{h\nu\eta_i} \left(\frac{\alpha_m + \langle\alpha_w\rangle}{\alpha_m} \right) \left(\frac{\gamma}{\gamma - \alpha_a} \right), \quad (1)$$

where A is the area (length times width) of the laser stripe, α_m is the mirror loss, $\langle\alpha_w\rangle$ is the modal loss in the waveguide (e.g., free-carrier absorption in the doped clads), e is the charge of the electron, $h\nu$ is the photon energy of the emitted light, and η_i is the internal quantum efficiency. D_{mode} is the width of the optical mode defined by $D_{\text{mode}} = D/\Gamma$ where D is the active region thickness and Γ is the optical confinement factor. $[(\gamma - \alpha_a)/J]$ is the only active region material parameter to appear in the threshold term of Eq. (1). The remaining parameters are related to the optical cavity and efficiency of electrical injection. When $[(\gamma - \alpha_a)/J]$ is maximized¹⁰ the threshold current is minimized.

Evaluation of this figure of merit, and knowledge of the net material gain (at the lasing wavelength) where that optimum ratio occurs $(\gamma - \alpha_a)_{\text{opt}}$, also allows us to determine the optimum thickness of the active region in midinfrared lasers as a function of mode width and modal losses. The rationale behind the traditional approach of thick active regions for interband lasers has been that the rapid increase of Auger recombination with carrier density makes high-density operation of the active regions unfavorable. This argument has also been suggested as a motivation for cascade structures.

Recent 2 μm lasers based on active regions with a few quantum wells, however, have produced high powers and operating temperatures. A five quantum well active region operated cw at room temperature¹¹ with a differential effi-

^{a)}Also with the Department of Physics and Astronomy.

^{b)}Electronic mail: flatte@rashi.physics.uiowa.edu

^{c)}Also with the Department of Electrical and Computer Engineering.

TABLE I. Results for ideal laser active region designs for seven systems at room temperature: band-gap E_g ; maximum net gain per unit volumetric current $[(\gamma - \alpha_a)/J]_{\max}$ and the net material gain $(\gamma - \alpha_a)_{\text{opt}}$, carrier density n_{opt} , and carrier lifetime τ at that optimum ratio of net gain to current density; optimum thickness of the active region D_{opt} and threshold current density J_{th} for a modal loss of $\alpha_m + \langle \alpha_w \rangle = 10 \text{ cm}^{-1}$ and a mode width $D_{\text{mode}} = 2 \text{ }\mu\text{m}$.

System	E_g (μm)	$[(\gamma - \alpha_a)/J]_{\max}$ ($\mu\text{m}^2/\text{A}$)	$(\gamma - \alpha_a)_{\text{opt}}$ (cm^{-1})	n_{opt} ($\times 10^{17} \text{ cm}^{-3}$)	τ (ns)	D_{opt} (\AA)	J_{th} (kA/cm^2)	$[(\gamma - \alpha_a)/\gamma]$
Superlattices								
I	15 \AA InAs/25 \AA Ga _{0.6} In _{0.4} Sb/ 15 \AA InAs/39 \AA Al _{0.30} Ga _{0.42} In _{0.28} As _{0.5} Sb _{0.5}	4.0	202	833.	10.0	0.39	240	0.990
II	20 \AA InAs/35 \AA Ga _{0.6} In _{0.4} Sb/ 20 \AA InAs/65 \AA Al _{0.30} Ga _{0.42} In _{0.28} As _{0.5} Sb _{0.5}	5.2	71	373	5.0	0.15	536	2.82
III	21 \AA InAs/31 \AA Ga _{0.7} In _{0.3} Sb/ 21 \AA InAs/43 \AA AlSb	4.0	206	560	7.5	0.45	357	0.971
Quantum wells								
IV	4.5 \times (15 \AA InAs/36 \AA Ga _{0.75} In _{0.25} Sb)/ 400 \AA Al _{0.20} Ga _{0.60} In _{0.20} As _{0.17} Sb _{0.83}	3.8	6.1	76	7.8	0.10	2630	32.6
V	100 \AA InAs _{0.85} Sb _{0.15} / 200 \AA In _{0.87} Al _{0.13} As _{0.91} Sb _{0.09}	3.8	96 ^a	109	4.0	0.56	1840	2.08
VI	80 \AA InAs _{0.88} Sb _{0.12} /80 \AA InAs _{0.76} P _{0.24}	4.4	39	221	6.3	0.18	907	5.08
Bulk								
VII	InAs	3.5	7.8	103	9.0	0.11	1940	25.8

^aIntersubband absorption for this structure at the lasing wavelength is substantially underestimated by calculations based on an eight-band bulk basis set. Thus, this number should be considered an overestimation of the figure of merit.

ciency of 36%. Cavities for these lasers had internal optical losses as low as 2 cm^{-1} . In view of this success we reconsider the issue of the optimal thickness of the active region in $4 \text{ }\mu\text{m}$ lasers. In brief, for active region materials with the highest gain to current ratio we find that the optimal thicknesses are much thinner than commonly grown.

We report calculations of the maximum net gain to current ratio $[(\gamma - \alpha_a)/J]_{\max}$, net material gain at that optimal point $(\gamma - \alpha_a)_{\text{opt}}$, and optimal thickness for seven structures at room temperature, detailed in Table I. These include two InAs/GaInSb/InAs/AlGaInAsSb superlattices,^{12,13} a $4.0 \text{ }\mu\text{m}$ InAs/GaInSb/InAs/AlSb superlattice,⁵ a $4.0 \text{ }\mu\text{m}$ superlattice multiple quantum well, two interband strained quantum wells (a $4.4 \text{ }\mu\text{m}$ InAsSb/InAsP structure² and a $4.0 \text{ }\mu\text{m}$ InAsSb/AlInAsSb structure¹⁴), and a bulk material (InAs). These results, listed in Table I, constitute the main quantitative results of this letter.

We now describe our calculations of the net material gain to volumetric current ratio, $[(\gamma - \alpha_a)/J]$, as a function of net gain. Calculations for the gain, intersubband absorption, and carrier recombination rates are performed with the full nonparabolic band structure and momentum-dependent matrix elements obtained from an eight-band bulk basis superlattice $\mathbf{K} \cdot \mathbf{p}$ formalism similar to Ref. 15 but generalized to an arbitrary number of layers in a superlattice unit cell. Input parameters¹⁶ to the calculation are limited to energy levels, matrix elements and effective masses of bulk constituents, and valence-band offsets between layers. This superlattice $\mathbf{K} \cdot \mathbf{p}$ formalism has been very successful in calculations of the optical properties¹⁷ and Auger rates of related type-II multilayer structures.

For systems II, IV, and VII, the Auger rates utilized were obtained optically by pump-probe differential transmission measurements.¹⁸ For system II, the $5.2 \text{ }\mu\text{m}$ wavelength four-layer superlattice,¹³ the Auger rate R_A can be written $R_A = Cn^2$, where n is the carrier density and $C = 2.5 \times 10^{-26} \text{ cm}^6/\text{s}$. For system IV, the superlattice multiple quantum well, $R_A = Cn^2/(1 + n/n_o)$ with $C = 7.8$

$\times 10^{-26} \text{ cm}^6/\text{s}$ and $n_o = 2 \times 10^{17} \text{ cm}^{-3}$.¹⁹ Bulk InAs has an Auger coefficient $C = 1.1 \times 10^{-26} \text{ cm}^6/\text{s}$.²⁰ The value of $9 \times 10^{-27} \text{ cm}^6/\text{s}$ for system V, a strained InAsSb quantum well, was obtained from photoconductivity measurements.¹⁴

For system VI, the InAsSb/InAsP quantum well, experimental numbers were not available. The multitude of valence subbands involved in the Auger rate calculation makes the calculations numerically intractable. Since the final states for Auger processes lie in the continuum, there is little difference between the density of states at zone center and at 0.2 \AA^{-1} . Hence, we calculate the density of states near the important final-state energies for Auger processes and evaluate the Auger rate using that information. The result is less accurate than our full calculations, but since the difference in the figure of merit between this system and the optimum systems is more than a factor of 5, this lessens our concern over the error. We note that we have used the band-gap value for InAs_{0.88}Sb_{0.12} taken from Ref. 2.

The Shockley-Read recombination time of high-quality samples of systems I, II, IV, and V is typically observed to be on the order of 3 ns. Thus, this rate is insignificant compared to the intrinsic Auger rate at the densities appropriate for laser operation. To compare the systems on an equal footing we assume a Shockley-Read lifetime of 3 ns for all systems.

In Fig. 1, $[(\gamma - \alpha_a)/J]$ is shown as a function of gain at 300 K for systems I, IV, VI, and VII of Table I. For each system at low gains and at high gains $[(\gamma - \alpha_a)/J]$ is small. At zero net gain the current density is the current required to maintain the transparency carrier density, and $[(\gamma - \alpha_a)/J] = 0$. At high gains the differential gain is small, requiring a large increase in the carrier density to increase the gain. Meanwhile, the current density is (roughly) proportional to n^3 (each of these systems is Auger-dominated over the entire range shown). In between low and high gains there is an optimal operation point for the active region where the net

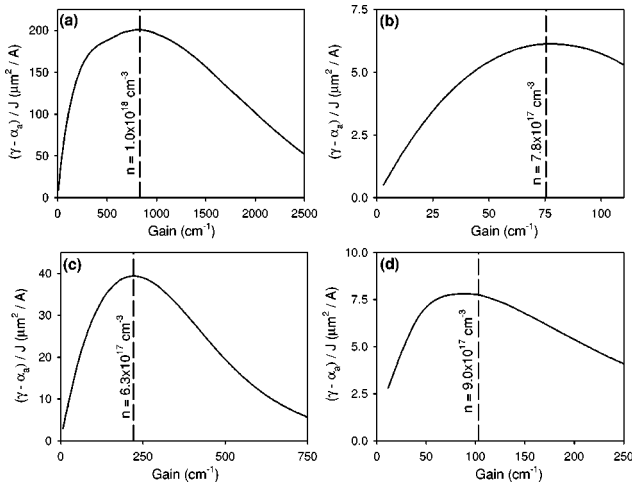


FIG. 1. Net gain per unit volumetric current $[(\gamma - \alpha_a)/J]$ as a function of net gain at 300 K for (a) system I, (b) system IV, (c) system VI, and (d) system VII. Note the different scales. Densities corresponding to the optimum $[(\gamma - \alpha_a)/J]$ are indicated in (a)–(d). Regardless of the laser cavity design, the active region should be operating at this optimum ratio for the lowest threshold current requirements.

gain per unit current density is the largest. In the case of system I this point occurs where the net material gain is 833 cm^{-1} , at a density roughly twice that of the transparency density.

Through evaluation of the maximum ratio of the net gain to the volumetric current density we can order the systems considered in terms of ideal laser performance. The optimized four-layer superlattices have the largest ratios of the systems considered. We note that systems I and III by this figure of merit appear to have essentially identical optimal performance. The quantum well systems have ratios five to ten times greater than bulk InAs.

We now evaluate the optimal thickness for the active region materials from

$$D_{\text{opt}} = D_{\text{mode}} \left(\frac{\alpha_m + \langle \alpha_w \rangle}{(\gamma - \alpha_a)_{\text{opt}}} \right). \quad (2)$$

Optimal active region thicknesses are shown in Table I for a low-loss midinfrared laser with a separate confinement region and coated facets: $D_{\text{mode}} = 2 \mu\text{m}$ and $(\alpha_m + \langle \alpha_w \rangle) = 10 \text{ cm}^{-1}$. Optimal thicknesses can be readily calculated for different waveguide parameters given the results in Table I. We find that the optimum active region thickness of four-layer superlattice materials is far thinner than commonly grown. In particular, for system I the threshold current density for a 3 period structure should be 3.3 times smaller than for a 40 period structure. The use of such a thin active region (240 \AA) necessitates a separate confinement structure to adequately confine the optical mode and minimize the penetration of the optical mode into the doped clad regions where optical losses are large. An additional benefit of the thin active region is that the transport properties of the device should improve.

The discussion to this point has focused on minimizing the threshold current. It can be seen from Eq. (1), however, that loss in the active region decreases the slope efficiency by the factor $(\gamma - \alpha_a)/\gamma$. This factor is shown in Table I evaluated at the density for which the net gain per unit current is

maximized. For all of the systems $(\gamma - \alpha_a)/\gamma$ is within 8% of its peak value (for systems I, II, and III it is within 1%) when the threshold current is minimized. Also, for all of the systems $(\gamma - \alpha_a)/\gamma$, and hence, the slope efficiency, can be increased by *reducing* the active region thickness. The active region thickness which maximizes the slope efficiency, however, differs only slightly from the thickness which minimizes the threshold current. In particular, for systems I, II, and III, where the intersubband absorption of the active region is very small at the lasing wavelength, the change in the desired active region thickness is less than 1%.

This research was supported in part by the U.S. Air Force, Air Force Materiel Command, Air Force Research Laboratory, Kirtland AFB, New Mexico, 87117-5777 (Contract No. F29601-97-C-0041), and the National Science Foundation (Grant No. ECS-9707799).

- ¹H. K. Choi, G. W. Turner, M. J. Manfra, and M. K. Connors, Appl. Phys. Lett. **68**, 2936 (1996).
- ²S. R. Kurtz, A. A. Allerman, and R. M. Biefeld, Appl. Phys. Lett. **70**, 3188 (1997).
- ³T. Ashley, C. T. Elliott, R. Jefferies, A. D. Johnson, G. J. Pryce, A. M. White, and M. Carroll, Appl. Phys. Lett. **70**, 931 (1997).
- ⁴D. H. Chow, R. H. Miles, T. C. Hasenberg, A. R. Kost, Y. H. Zhang, H. L. Dunlap, and L. West, Appl. Phys. Lett. **67**, 3700 (1995); T. C. Hasenberg, R. H. Miles, A. R. Kost, and L. West, IEEE J. Quantum Electron. **33**, 1403 (1997).
- ⁵J. I. Malin, J. R. Meyer, C. L. Felix, J. R. Lindle, L. Goldberg, C. A. Hoffman, and F. J. Bartoli, Appl. Phys. Lett. **68**, 2976 (1996).
- ⁶L. J. Olafsen, E. H. Aifer, I. Vurgaftman, W. W. Bewley, C. L. Felix, J. R. Meyer, D. Zhang, C.-H. Lin, and S. S. Pei, Appl. Phys. Lett. **72**, 2370 (1998).
- ⁷J. Faist, F. Capasso, D. L. Sivco, C. Sirtori, A. L. Hutchinson, and A. Y. Cho, Science **264**, 553 (1994).
- ⁸M. E. Flatté, C. H. Grein, H. Ehrenreich, R. H. Miles, and H. Cruz, J. Appl. Phys. **78**, 4552 (1995).
- ⁹C. H. Grein, P. M. Young, and H. Ehrenreich, J. Appl. Phys. **76**, 1940 (1994).
- ¹⁰See, e.g., L. A. Coldren and S. W. Corzine, *Diode Lasers and Photonic Integrated Circuits* (Wiley, New York, 1995).
- ¹¹D. Z. Garbuzov, R. U. Martinelli, H. Lee, P. K. York, R. J. Menna, J. C. Connolly, and S. Y. Narayan, Appl. Phys. Lett. **69**, 2006 (1996).
- ¹²M. E. Flatté, J. T. Olesberg, S. A. Anson, T. F. Boggess, T. C. Hasenberg, R. H. Miles, and C. H. Grein, Appl. Phys. Lett. **70**, 3212 (1997).
- ¹³M. E. Flatté, T. C. Hasenberg, J. T. Olesberg, S. A. Anson, T. F. Boggess, C. Yan, and D. L. McDaniel, Jr., Appl. Phys. Lett. **71**, 3764 (1997).
- ¹⁴J. R. Lindle, J. R. Meyer, C. A. Hoffman, F. J. Bartoli, G. W. Turner, and H. K. Choi, Appl. Phys. Lett. **67**, 3153 (1995).
- ¹⁵M. E. Flatté, P. M. Young, L.-H. Peng, and H. Ehrenreich, Phys. Rev. B **53**, 1963 (1996).
- ¹⁶Parameters for the systems considered come from *Physics of Group IV Elements and III-V Compounds*, Landolt-Börnstein Vol. III/17a, edited by O. Madelung (Springer, New York, 1982); *Intrinsic Properties of Group IV Elements and III-V, II-VI, and I-VII Compounds*, Landolt-Börnstein Vol. III/22a, edited by O. Madelung (Springer, New York, 1987); many of them are tabulated in Ref. 8.
- ¹⁷J. T. Olesberg, S. A. Anson, S. W. McCahon, M. E. Flatté, T. F. Boggess, D. H. Chow, and T. C. Hasenberg, Appl. Phys. Lett. **72**, 229 (1998).
- ¹⁸See, e.g., S. W. McCahon, S. A. Anson, D.-J. Jang, M. E. Flatté, T. F. Boggess, D. H. Chow, T. C. Hasenberg, and C. H. Grein, Appl. Phys. Lett. **68**, 2135 (1996).
- ¹⁹The density convention used here for quantum well systems is to include both the barrier and well material in the thickness of the material.
- ²⁰K. L. Vodopyanov, H. Graener, C. C. Phillips, and T. J. Tate, Phys. Rev. B **46**, 13194 (1992).